X-601-76-294
PREPRINT

TMX 71272

WORST CASE SPACE RADIATION ENVIRONMENTS FOR GEOCENTRIC MISSIONS

E. G. STASSINOPOULOS
S. M. SELTZER

DECEMBER 1976

GODDARD SPACE FLIGHT CENTER
GREENBELT, MARYLAND

WORST-CASE SPACE RADIATION EXPOSURE FOR GEOCENTRIC MISSIONS

E. G. Stassinopoulos
NASA/Goddard Space Flight Center
Greenbelt, Maryland 20771

S. M. Seltzer
National Bureau of Standards
Washington, D.C. 20234

Summary

Worst-case possible annual radiation fluences of energetic charged particles in the terrestrial space environment, and the resultant depth-dose distributions in aluminum, have been calculated in order to establish absolute upper limits to the radiation exposure of spacecraft in geocentric orbits. The results are a concise set of data intended to aid in the determination of the feasibility of a particular mission. The data may further serve as guidelines in the evaluation of standard spacecraft components.

Calculations were performed for each significant particle species populating or visiting the magnetosphere, on the basis of volume occupied by or accessible to the respective species. Thus, magnetospheric space was divided into five distinct regions (see Figure 1) using the magnetic shell parameter L, which gives the approximate geocentric distance (in earth radii) of a field line's equatorial intersect (note that the physical relevance of L gradually deteriorates for equatorial distances greater than 5-6 earth radii because of solar-wind-to-magnetosphere interaction-effects).

An arrangement corresponding to that of Figure 1 but in polar R-Λ space is shown in Figure 2. The dipole field-line equation ($R=L\cos^2\Lambda$) was used to map the domains, where R is radial distance and Λ is invariant latitude.

The indicated domain boundaries, in either reference frame, should be considered only approximate transition areas, not lines; they are assumed for modelling purposes and, additionally, are used here to convey a qualitative picture of the charged particle distribution. Respective "real" boundaries, if such could be found and defined, would most likely be diffuse areas fluctuating in their L positions due to several factors, such as magnetic perturbations (storm and substorm effects), local time effects (diurnal variation), solar cycle variation (minimum and maximum activity phases), individual solar events, etc., and would furthermore vary with particle energy.

Energetic Van Allen belt electrons are distinguished into "inner zone" and "outer zone" populations, occupying respectively regions #1 and #2-3-4. The L=2.8 line is being used to separate the inner and outer zone domains, while the termination of the outer zone at L=12 earth radii is intended only to delineate the maximum outward extent of stable or pseudo electron trapping.

Energetic Van Allen belt protons are usually contained within a dipole shell of about L=4 earth radii. The precise volume occupied by these particles depends inversely on their energy. Shown in Figures 1 and 2 are protons with energies E>5 Mev populating regions #1 and #2 with an approximate trapping domain boundary placed at L=3.8 earth radii.

Finally, the solar flare proton domain is shown in Figures 1 and 2 to extend over regions #4 and #5. It was evaluated without rigorous rigidity considerations by assuming that particles of all energies above 10 Mev have free access to a geomagnetic cutoff latitude of 63 degrees, which corresponds to an L value of about 5 earth radii.

The particle radiation results of our calculations are given in Table 1 for each species. All data represent integral, omnidirectional, annual fluences in units of particles per square centimeter. In order to obtain truly worst case estimates, the uncertainty factors associated with the environment models were applied to the data. Also the outer zone electron fluxes were adjusted in the high energy range of the spectrum (E>1 Mev) by raising the intensities above model predictions so as to reflect latest experimental findings. Solar proton fluences are unattenuated, interplanetary intensities of anomalously large events at 1 AU, determined statistically as functions of mission duration and confidence level.

The doses for electrons were obtained from Monte Carlo electron-photon transport calculations for aluminum targets (density 2.70 gm/cm^3) exposed to monenergetic, isotropic fluxes. The monoenergetic results were smoothed and scaled so as to facilitate interpolation and integration for any spectrum. Although the effects of Bremsstrahlung production were included in the results, the calculations were not made in a way suitable to obtain the depth-dose distribution in the region of deep penetration (Bremsstrahlung tail). The present results describe the dose only up to depths about equal to the mean range of the electrons. Separate calculations for the Bremsstrahlung dose are presently being carried out.

For protons, a simpler approach is sufficient. Assuming straight ahead penetration and continuous energy loss, depth-dose distributions were calculated for monoenergetic, isotropic fluxes. As in the case of electrons, the monoenergetic proton results were incorporated into a procedure to rapidly perform the integration over arbitrary spectra.

Depth-dose distributions for the spectra of Table 1 are given in Figure 3. Because portions of the calculations are still underway, the present results are somewhat tentative and must be considered preliminary.

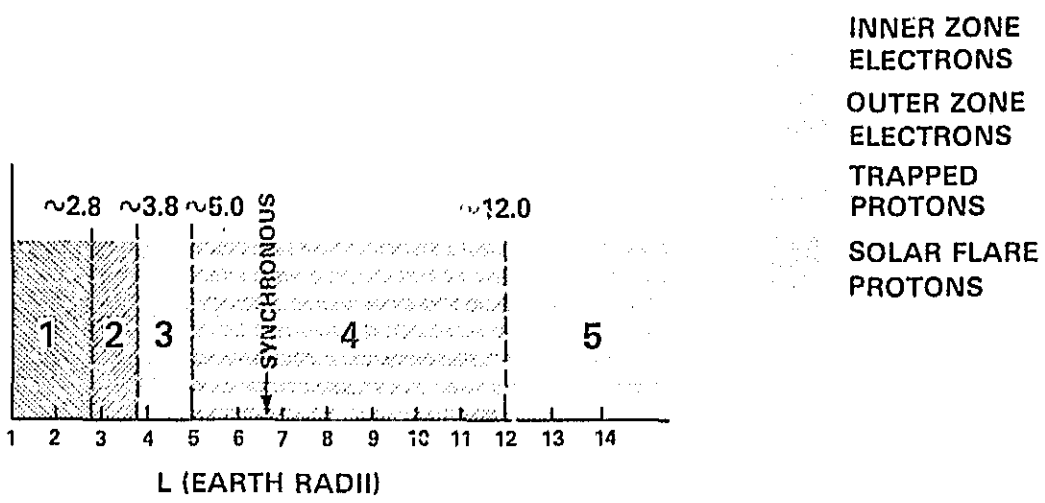

FIGURE 1: APPROXIMATE SPECIES DOMAINS IN MAGNETIC L SPACE

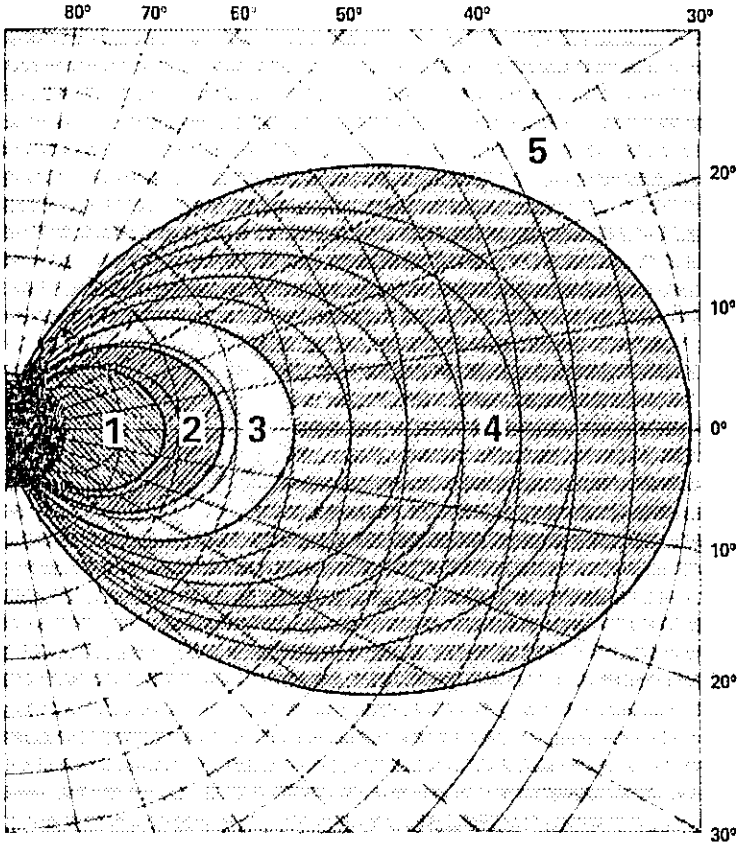

FIGURE 2: APPROXIMATE SPECIES DOMAINS IN POLAR R—Λ SPACE

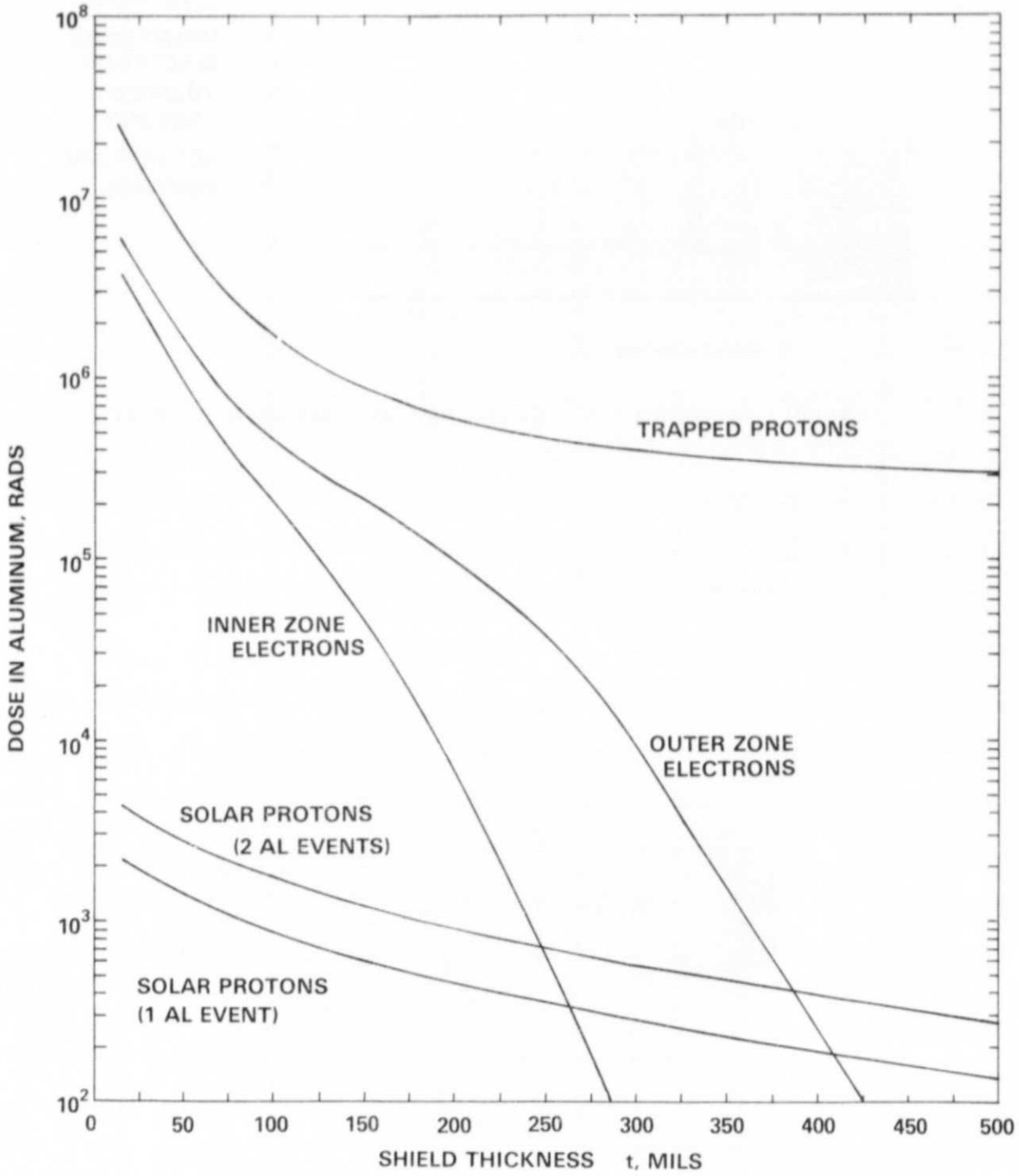

FIGURE 3: DEPTH DOSE DISTRIBUTION FOR WORST-CASE RADIATION PREDICTIONS IN $RADS_{AL}$

TABLE 1

ENERGETIC CHARGED PARTICLE SPACE RADIATION: EARTH ENVIRONMENT

WORST CASE PREDICTIONS OF OMNIDIRECTIONAL, INTEGRAL FLUENCES FOR A MISSION DURATION OF T =1 YEAR DURING A PERIOD OF MAXIMUM SOLAR ACTIVITY

TERRESTRIAL RADIATION BELT: ANNUAL TRAPPED PARTICLE FLUENCES					UNATTENUATED INTERPLANETARY SOLAR FLARE PROTON FLUENCES AT 1 AU		
	ELECTRONS		PROTONS			CONFIDENCE LEVEL Q (%)	
	INNER ZONE	OUTER ZONE				80–95	96–99
E(>MEV)	(e/cm^2)	(e/cm^2)	E(>MEV)	(P/cm^2)	E(>MEV)	(P/cm^2)	(P/cm^2)
1.0	1.31E 14	2.183E 14	5	1.073E 15	10	1.680E 10	3.360E 10
1.5	5.04E 13	9.235E 13	10	1.627E 14	20	1.152E 10	2.304E 10
2.0	2.41E 13	4.198E 13	15	5.417E 13	30	7.900E 09	1.580E 10
2.5	1.10E 13	3.232E 13	20	2.482E 13	40	5.417E 09	1.083E 10
3.0	1.79E 12	2.770E 13	25	1.358E 13	50	3.714E 09	7.428E 09
3.5	1.75E 11	1.956E 13	30	1.022E 13	60	2.547E 09	5.094E 09
4.0	1.49E 10	8.563E 12	40	9.490E 12	70	1.746E 09	3.492E 09
4.5	1.20E 09	1.931E 12	50	8.687E 12	80	1.197E 09	2.394E 09
5.0	5.20E 07	2.057E 11	60	7.884E 12	90	8.210E 08	1.642E 09
5.5	1.70E 06	8.395E 09	80	6.563E 12	100	5.629E 08	1.126E 09
6.0	3.00E 04	3.000E 05	100	5.439E 12			
						NO. OF AL EVENTS PREDICTED FOR GIVEN T & Q	
						1	2